# LIGHT DIFFRACTION STUDY OF SINGLE SKELETAL MUSCLE FIBERS

R. J. BASKIN, *Department of Zoology, University of California, Davis, California 95616*
K. P. ROOS, *Cardiovascular Research Laboratory, University of California, Los Angeles School of Medicine, Los Angeles, California 90024*
Y. YEH, *Department of Applied Science, University of California, Davis, California 95616 U.S.A.*

ABSTRACT Light diffraction patterns from isolated frog semitendinosus muscle fibers were examined. When transilluminated by laser light, the muscle striations produce a diffraction pattern consisting of a series of lines that are projected as points onto an optical detector by a lens system. Diffraction data may be sequentially stored every 18 ms for later processing by digital computer systems. First- and second-order diffraction line intensities were examined from intact, chemically skinned, and glycerinated single fibers. The diffraction line intensities demonstrated a strong length dependence upon passive stretch from reference length to 3.6 $\mu$m. The first-order intensity linearly increased an average of 15-fold over the range examined. The magnitude of the second order intensity was less than the first order and showed an exponential rise with increasing length. Both first- and second-order intensities decreased upon muscle activation. Data from chemically skinned and glycerinated single fibers were not significantly different from intact fibers, indicating that the membrane structure has little effect upon the diffraction phenomenon in muscle. Theoretical model systems are examined in an attempt to find the basis of these results. Neither an analysis based on a diffraction grating with variable spacing nor the unit cell model of Fujime provides an explanation for the observed length dependency of intensity. Though the origin of the intensity decrease upon stimulation is not known, we have suggested that it could result from lateral misalignment of myofibrils that can occur upon activation.

## INTRODUCTION

Due to the presence of a regular array of alternating light and dark bands (A and I bands), single striated muscle fibers act as a one-dimensional diffraction grating when illuminated by monochromatic light (Sandow, 1936*a*). Striated muscle was first used as a transmission grating by Ranvier (1874). He was able to observe a divergence in the lateral orders of the diffraction pattern during contraction and concluded that the "discus sarcous-elements" had moved together. Sandow (1936*a*, b) investigated diffraction patterns in frog sartorius muscles during both stretch and contraction.

Buchthal and Knappeis (1940) were the first to investigate diffraction spectra using isolated single fibers. They measured the grating constant (sarcomere length) and intensity distribution in both whole muscle and single fibers. They found that while the grating constant was the same in both whole and single fibers, the intensity distribution and its change under extension and contraction differed.

Hill (1953*a*, *b*) was the first to show a decrease in the intensity of light diffracted by frog

striated muscle during activation. Cleworth and Edman (1972) and Kawai and Kuntz (1973) developed methods for the rapid recording of light diffraction patterns. A possible explanation of the intensity changes of the diffraction lines for a resting muscle at various sarcomere lengths was provided by the theoretical development of Fujime (1975). His experimental results, which showed little change in the intensity of the first-order line with change in sarcomere length, coincided with his theoretical analysis. He also observed a large drop in the intensity of the first-order line upon stimulation as did Halpern (1977) and Zite-Ferenczy and Rudel (1978).

With a slit source and a one-dimensional grating, a series of diffraction lines corresponding to various orders are observed. With a spot source, however, a series of diffraction spots each corresponding to a different diffraction order results. Thus, it would be expected that a spot pattern would result from a laser beam incident onto a muscle fiber. However, the diffraction lines that are observed result also from an edge effect of individual muscle fibers. This results in a series of diffraction lines, the "spot" having spread due to the edge effect of fibers. (A similar effect could be expected from the edges of individual myofibrils. This appears to be unlikely, however, because it is difficult to observe myofibril edges unless the muscle fiber itself is extensively disrupted.)

In recent work we have developed rapid methods for examining light diffraction patterns at rest and during activity (Paolini et al., 1976; Paolini et al., 1977). We have examined sarcomere length dispersion and made preliminary measurements of the variation in first-order line intensity with sarcomere length.

In the present investigation we examine in detail the sarcomere length dependence of the first- and second-order line intensities of intact, chemically skinned and glycerinated resting and activated single frog striated muscle fibers. We also discuss briefly a theoretical model from which we predict changes in the intensity of the first- and second-order diffraction lines for a (three-dimensional) muscle fiber.

## LIST OF SYMBOLS

| | |
|---|---|
| $A$ | Empirically derived optical system constant. |
| $a$ | Radius of diffracting cylinder. |
| $a'$ | Wave amplitude. |
| $B$ | Empirically derived optical system constant. |
| $b$ | Width of $I$-band. |
| $C$ | Collector system. |
| $h'$ | Output displacement. |
| $I$ | Line intensity. |
| $J_1(X)$ | Bessel function of the first order for the argument $X$. |
| $K$ | Position of zero-order peak. |
| $M$ | Magnification factor. |
| $n$ | Diffracted order. |
| $N$ | Number of slits (sarcomeres) in a plane grating. |
| $N_s$ | Refractive index of saline. |
| $q_p$ | Equatorial component of the scattering wave vector. |
| $R$ | Relay cylinders. |

$S$ Sarcomere length.
$S_t$ Stigmatizing cylinders.
$V_o$ Sarcomere volume.
$x$ Distance from fiber to recording device.
$X_p$ Position of analyzed peak.
$\alpha$ Input angle.
$\beta$ $\pi b \sin \theta/\lambda$.
$\gamma$ $\pi d \sin \theta/\lambda$.
$\lambda$ Wavelength of light.
$\theta$ Diffraction angle.

## MATERIALS AND METHODS

Experimental preparation: Semitendinosus muscles from double-pithed northern grass frogs *(Rana pipiens)* are excised and dissected as previously described (Paolini et al., 1977) on a microscope slide in chilled saline. If the dissected fiber, after equilibrating 30 min, shows no opaque regions that would indicate fiber damage, small foil clips are wrapped around the tendon close to the point of fiber attachment and the remainder of the tendon is clipped off (Ford et al., 1977). The microscope slide with the fiber is mounted directly into a milled slot on the cooled muscle chamber base. The top half of the chamber is placed over the base and sealed so that the fiber lies in a narrow (3 mm) trough containing fresh circulating saline. The pin of a low compliance strain gauge force transducer is attached to one end of the fiber; the other end is connected to a hooked pin at the end of a pen motor rack and pinion. The rack position and thus muscle length is indicated by a proximity transducer. The chamber top contains two parallel platinum electrodes used to stimulate the muscle fiber.

### *Optical System*

A 1-MW HeNe laser CW Radiation, Inc., Pittsburgh, Pa. mounted vertically irradiates the single fiber through the glass slide (see Fig. 1). Incident intensity is controlled by crossed polarizing filters; the upper polarizer is fixed in orientation so that the plane of polarization incident upon the fiber is constant. To increase the portion of the diffraction cone that was collected and measured it was necessary to develop a new optical system. The new system, which is discussed in Appendix I, can collect light from a half-angle of 80° with a usable working distance of ~0.83 mm. This allows 89% of the equatorial extent of the diffraction pattern from the fiber to be collected and condensed into a series of points, each representing one diffraction line. The diffraction image is focused upon the window of a 256-element charge-coupled device (CCD) photosensor array that is controlled by a dual-channel diffractometer (Paolini et al., 1976). Video data from the diffractometer is amplified, digitized, and sequentially stored in the memory of a PDP-8 computer (Digital Equipment Co., Marlboro, Mass.) as a single 256-point waveform or as a series of up to 10 waveforms. In the present configuration, the analog-to-digital conversion rate allowed for a scan rate of 18 ms/waveform. The stimulator can be turned on and off either manually or under computer control as required by a given experiment. Muscle position and tension are simultaneously recorded on a storage oscilloscope.

### *Data Analysis*

Diffraction data waveforms stored in the PDP-8 computer memory may be selectively displayed. Data is transferred to the memory of an Intel 8080 microprocessor (Intel Corp., Santa Clara, Calif.) based microcomputer system for analysis. The waveforms may be photographed directly off the display cathode ray tube terminal or drawn on a $X$-$Y$ plotter for permanent storage. Each waveform is analyzed by the microcomputer and values for sarcomere length (peak position), intensity, line width, and dispersion are determined.

The CCD photosensor can be moved along an axis parallel to the fiber so that the desired portion of

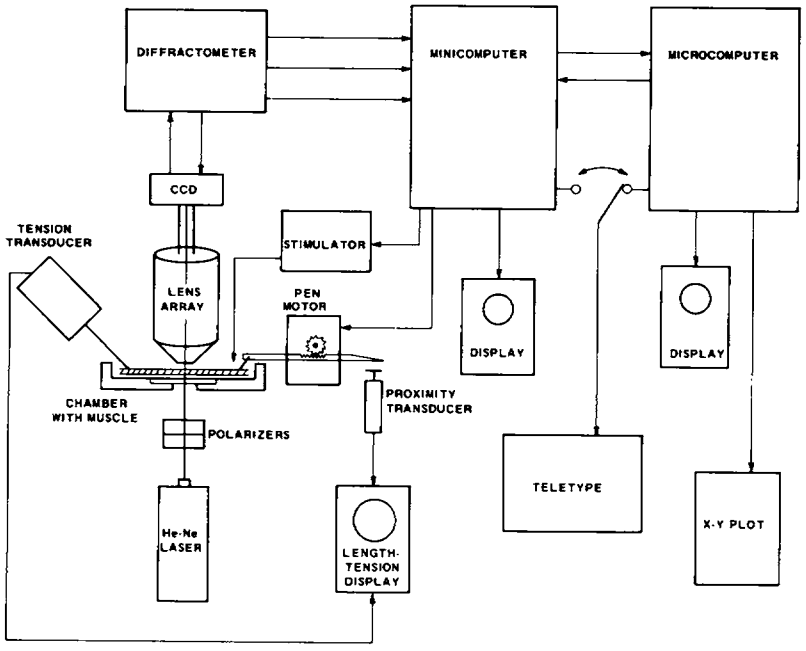


FIGURE 1 Diagram of a diffraction system. Details of the optical system are presented in the Appendix. The CCD sensor has been described by Paolini et al. (1976). The minicomputer is a PDP-8 system and the microcomputer is an Intel 8080 based system. Both computer displays are Tektronix 502 oscilloscopes (Tektronix, Inc., Beaverton, Oreg.); the length-tension display is a Tektronix 564 storage oscilloscope. See text for further details.

the diffraction spectra can be examined for a given experiment. After the photosensor is locked in place, its position is calibrated using precision transmission gratings (Bausch & Lomb, Inc., Rochester, N.Y.) in place of the muscle (1.89, 2.50, 2.77, and 3.33 $\mu$m). Sarcomere length ($S$) can then be calculated using the grating equation modified for the geometry of this optical system:

$$S = \frac{n\lambda}{N_s \sin\left[AM(K + X_p) - B\right]},$$

where $n$ = the diffracted order (0, 1, 2, etc.); $\lambda$ = wavelength of light (0.6328 $\mu$m); $N_s$ = index of refraction of saline (1.3345); $A$, $B$ = empirically derived constants for this optical system; $M$ = calibrated magnification factor; $K$ = calibrated position of the zero-order peak; $X_p$ = position of analyzed peak. The intensity of the first- and second-order diffraction lines is determined by summing the output of those CCD elements falling between boundary cursors set to delimit the output waveform. (All of the array elements with a level above the background are summed to give the intensity value for a diffraction order.) The photosensor dark current is determined several times during the course of an experiment and is subtracted from the output waveform.

### *Focused Diffraction Orders*

The focused diffraction order is elliptically shaped and is ~78 $\mu$m long by 27 $\mu$m wide at a $S$ of 2.6 $\mu$m. The photodiode strip is 17 $\mu$m wide and 3,328 $\mu$m long. A slight widening of the focused diffraction order is seen at greater $S$. This results in a slight underestimation of $I_1$ and $I_2$ at long $S$. For each data point the detector is set for maximum intensity. It may be moved laterally ~10 $\mu$m without registering an intensity change.

### *Procedure*

First- and second-order diffraction patterns have been examined from 32 intact (at rest and tetanically stimulated), 6 chemically skinned (at rest and chemically activated), and 7 glycerinated single fibers. Intact single muscle fibers were prepared by dissection as previously described. Only data from intact fibers that were viable throughout the several-hour duration of each experiment and yielded good diffraction patterns over a wide range of $S$ were used. Chemically skinned muscle fibers were prepared from intact single fibers by the Julian (1971) method of partial glycerination. To activate these chemically treated fibers, the relaxing solution of Julian (1971) is temporarily replaced by a contracting solution with a low PCa of 6.09 to insure complete activation. Glycerinated muscle fibers are prepared from intact fibers by placing them in a glycerol:water (1:1) solution in the freezer for several weeks. Before each experiment, the glycerinated fibers are equilibrated in a relaxing solution for 24 h.

The first data waveform taken for every experiment is from a resting muscle at its shortest length. All subsequent intensity data is recorded relative to this first point. The muscle fiber is positioned for each data waveform so that the intensity of the diffraction peak is at a maximum. Intensity data is taken as the fiber is incrementally stretched in a series of steps from both ends to maintain the same portion of the fiber in the laser beam. After the initial resting series of waveforms, the fiber is returned to its shortest length. The entire series may then be repeated, or the fibers tetanically stimulated or chemically activated at each length step. Extreme care is taken to insure that the fiber remains properly positioned in the laser beam when activated.

## RESULTS

### *Dependence of First-Order Line Intensity upon S*

We first examined closely the variation of first-order line intensity with $S$. Our earlier results had shown a dependence of first-order line intensity upon $S$. However, the optical system we used did not gather a large fraction of the light in the diffraction cone. As indicated earlier, our present optical system was designed to remedy this problem.

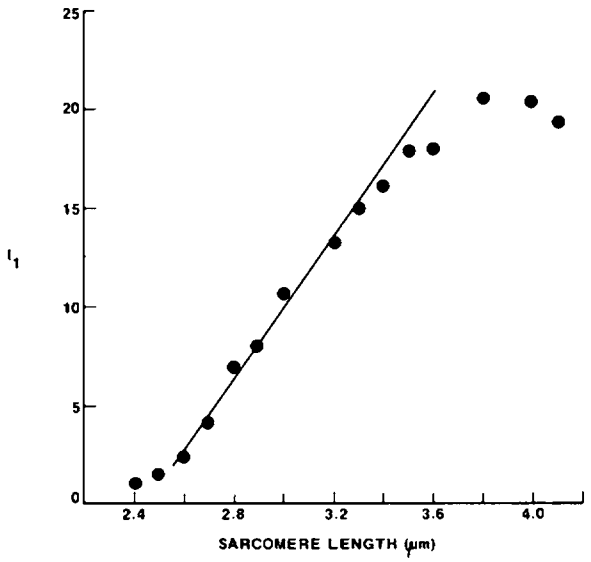


FIGURE 2 Dependence of first-order line intensity upon $S$. Muscle No. 128. The line represents a least squares fit from 2.5 to 3.5 μm. Vertical axis intensity units are relative to the arbitrary chosen value of 10 U at a $S$ of 3.0 μm.

Using isolated single fibers, the intensity of the first-order diffraction line was found to be a function of $S$. In some experiments an intensity change of >15-fold was found over the range of $S$ from 2.4 to 3.6 $\mu$m (Fig. 2).

Variability was often noted from one fiber to the next. (For a few experiments [<20% of the total] the linear dependence of first-order line intensity upon $S$ terminated at $S$ from 3.0 to 3.6 $\mu$m.) To best characterize our results we have tabulated data (Table I) of 13 experiments from 11 intact muscle fibers whose coefficients of determination ($r^2$) exceeded 0.900 ($r^2$ = 1.000 indicates best fit). Several muscles were examined more than once, and their results are indicated separately. For each run listed in Table I we have tabulated the range of $S$ examined, the number of separate determinations (points), the regression coefficients $a_0$ and $a_1$ for a least squares fit ($y = a_0 + a_1 x$) to the data, and the coefficient of determination ($r^2$). The range in values of the intercept ($a_0$) and the slope ($a_1$) found in various runs may represent variability inherent in our methods or in the fiber preparations.

The first-order regression coefficients of 13 intact fiber experiments were averaged, and the intercept ($a_0$) was found to be $-24.94 \pm 7.00$ arbitrary intensity U, whereas the slope ($a_1$) averaged $11.60 \pm 2.30$ arbitrary intensity U/$\mu$m. Averaged linear regression data from chemically skinned (both before and after skinning) and glycerinated fiber preparations also demonstrate similar length dependencies as shown in Table II. Only regression coefficients from experiments whose coefficients of determination were in excess of 0.900 were averaged. There is no significant difference in the averaged regression coefficients between resting intact, chemically skinned, and glycerinated single fibers. In all cases, a strong dependence of first-order line intensity upon $S$ is found.

*Dependence of Second-Order Line Intensity upon S*

The second-order line was, on the average, much less intense than the first-order line; however, it also showed a strong dependence on $S$. Second-order line intensity generally

TABLE I
DEPENDENCE OF FIRST-ORDER LINE INTENSITY UPON $S$

| Muscle | Experimental range | Points | Least squares fit | | |
|---|---|---|---|---|---|
| | | | $a_0$ | $a_1$ | $r^2$ |
| *n* | $\mu m$ | *n* | | | |
| 73 | 2.65–3.69 | 7 | −23.39 | 11.13 | 0.928 |
| 76 | 2.27–3.47 | 7 | −19.97 | 9.99 | 0.948 |
| 101 | 2.29–3.36 | 6 | −37.29 | 15.77 | 0.981 |
| 124(1) | 2.28–3.12 | 9 | −16.60 | 8.87 | 0.900 |
| 124(2) | 2.36–3.12 | 8 | −34.68 | 14.89 | 0.928 |
| 126(2) | 2.09–3.00 | 7 | −24.24 | 11.41 | 0.929 |
| 128(1) | 2.50–3.50 | 11 | −25.56 | 11.54 | 0.913 |
| 128(2) | 2.36–3.50 | 10 | −27.91 | 12.07 | 0.929 |
| 133 | 2.51–3.40 | 9 | −34.93 | 14.98 | 0.967 |
| 134(2) | 2.94–3.46 | 6 | −18.15 | 9.38 | 0.915 |
| 145 | 2.78–3.74 | 8 | −24.71 | 11.57 | 0.926 |
| 152 | 2.00–2.86 | 8 | −17.00 | 9.20 | 0.944 |
| 153(2) | 2.20–3.57 | 15 | −19.84 | 9.95 | 0.934 |

$r^2$ is the coefficient of determination where $r^2$ = 1.00 would indicate best fit.

TABLE II
LENGTH–INTENSITY DATA SUMMARY

| Type of experiment | Order | Experiments | Significantly different | Type of regression | Average regression coefficients | |
|---|---|---|---|---|---|---|
| | | | | | Coefficient* | Coefficient‡ |
| | | *n* | | | *U* | *U/μm* |
| Intact fibers | | | | | | |
| At rest | First | 13 | — | Linear | $-24.94 \pm 7.00$ | $11.60 \pm 2.30$ |
| Stimulated fibers at rest | First | 5 | No§ | Linear | $-20.32 \pm 7.17$ | $9.96 \pm 2.21$ |
| Stimulated fibers | First | 5 | Yes§ | Linear | $-11.60 \pm 13.09$ | $5.26 \pm 5.03$ |
| At rest | Second | 4 | — | Exponential | $2.53 \pm 2.26 \times 10^{-3}$ | $2.26 \pm 0.66$ |
| Stimulated fibers at rest | Second | 2 | No‖ | Exponential | $3.94 \pm 0.58 \times 10^{-3}$ | $1.88 \pm 0.10$ |
| Stimulated fibers | Second | 2 | No‖ | Exponential | $3.38 \pm 2.10 \times 10^{-3}$ | $1.77 \pm 0.06$ |
| Chemically skinned | | | | | | |
| Intact at rest | First | 5 | No§ | Linear | $-20.34 \pm 7.33$ | $10.17 \pm 2.47$ |
| Skinned relaxed | First | 6 | No§ | Linear | $-26.57 \pm 16.23$ | $13.44 \pm 6.86$ |
| Glycerinated fibers | | | | | | |
| Relaxed | First | 4 | No§ | Linear | $-22.73 \pm 4.33$ | $10.94 \pm 1.50$ |
| Relaxed | Second | 1 | No‖ | Exponential | $2.63 \times 10^{-4}$ | 2.75 |

$a_0$ and $a_1$ are regression coefficients for a least squares fit and $a$ and $b$ coefficients for an experimental fit.
*Designated as $a_0$ for linear regression analysis and $a$ for exponential analysis.
‡Designated as $a_1$ for linear regression analysis and $b$ for exponential analysis.
§Compared to base mean value for first order.
‖Compared to base mean value for second order.

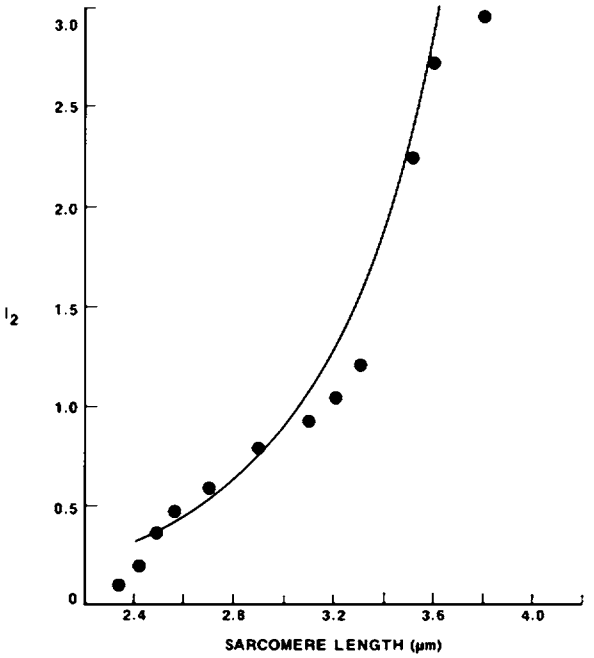


FIGURE 3 Dependence of second-order line intensity upon sarcomere length. Muscle No. 139. Curve represents an exponential fit to the points. Vertical axis intensity units are the same as in Fig. 2 and indicate that second-order line intensity is nearly 10-fold below first-order line intensity at the correspondings.

TABLE III
DEPENDENCE OF SECOND-ORDER LINE INTENSITY UPON $S$

| Muscle | Experimental range | Points | Exponential fit | | |
|---|---|---|---|---|---|
| | | | $a$ | $b$ | $r^2$ |
| 94 | 2.52–3.71 | 5 | $7.84 \times 10^{-4}$ | 2.38 | 0.816 |
| 97 | 2.45–3.44 | 6 | $1.43 \times 10^{-3}$ | 2.18 | 0.907 |
| 106 | 2.80–3.78 | 6 | $5.66 \times 10^{-6}$ | 4.03 | 0.895 |
| 109 | 2.30–3.78 | 11 | $6.46 \times 10^{-5}$ | 3.22 | 0.957 |
| 139(1) | 2.27–3.59 | 12 | $5.23 \times 10^{-3}$ | 1.75 | 0.918 |
| 139(2) | 2.29–3.54 | 12 | $3.40 \times 10^{-3}$ | 1.90 | 0.910 |
| 141(1) | 2.06–2.28 | 9 | $4.11 \times 10^{-4}$ | 2.60 | 0.801 |
| 141(2) | 2.03–2.70 | 12 | $3.12 \times 10^{-6}$ | 4.23 | 0.807 |

$a$ and $b$ are regression coefficients for an exponential fit, and $r^2$ is the coefficient of determination where $r^2 = 1.00$ would indicate best fit.

showed a best fit to an exponential function $y = ae^{bx}$, where $a$ and $b$ are regression coefficients. The dependence of second-order line intensity upon $S$ is shown in Fig. 3 for experiment 139-1. Exponential regression coefficients have been tabulated for eight experiments from six intact fibers (Table III). Averaged values from the four best fit regression data ($r^2 > 0.900$) are tabulated along with the second-order glycerinated fiber data in Table II. There is no significant difference in second-order resting coefficients.

*Variation in First-Order Line Intensity upon Stimulation*

Stimulation of the fiber results in a large decrease in the intensity of the first-order line. The decrease is less at short $S$ than at longer lengths (Fig. 4). Linear regression coefficients from

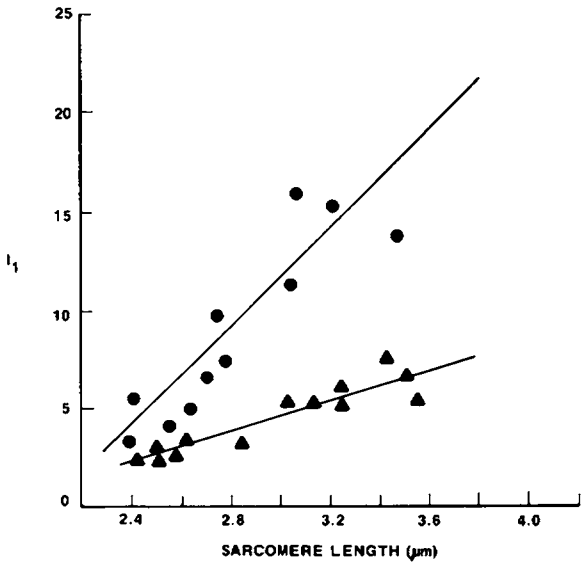


FIGURE 4 First-order line intensity as a function of $S$ in an active fiber. Muscle No. 138. Lines represent least squares fit for changes at rest (●) and during tetanic contraction (▲). Vertical intensity axis units are the same as in Fig. 2.

five experiments on intact fibers are averaged and compared to other experiments in Table II. In each of the five separate fibers a determination was first made of the change in first-order line intensity with $S$ for a muscle fiber at rest. The variation upon stimulation in each fiber was then measured. The magnitude of the decrease varied from ~30% at a $S$ of 2.4 $\mu$m to over 60% at a 3.4-$\mu$m $S$. There was a significant difference between the averaged regression coefficients from fibers during tetanus and those from resting or relaxed fibers. It should also be noted that the first-order intensity of activated chemically skinned fibers dropped 30–65% from relaxed values. (There were too few data points from each experiment to calculate a regression slope accurately.)

*Variation in Second-Order Line Intensity upon Stimulation*

Second-order line intensity showed a much less dramatic change upon stimulation than did the first-order line (Table II). The average of these experiments given in Table II indicated an insignificant intensity decrease upon activation. A larger decrease in the second-order line intensity is generally observed upon stimulation; however, when allowance is made for a slight decrease in $S$, it is found that the observed intensity is close to the resting value at the new length. (Due to the steepness of the second-order curve, a small change in length results in a large change in line intensity.)

## DISCUSSION

The major result of this investigation is that first- and second-order line intensities show a strong dependence upon $S$. Table IV summarizes the results of earlier measurements of the intensity in both resting and active muscle. The large variation in length dependency of intensity data is due to the many different types of muscle preparations, detection systems,

TABLE IV
DIFFRACTION INTENSITY CHANGES

| Investigator | Resting Muscle | | Active muscle |
|---|---|---|---|
| | First-order line | Second-order line | First-order line |
| Sandow (1936 *a,b*) | Decrease | No change | No change |
| Buchthal and Knappeis (1940)* | Increase | — | No change |
| Hill (153 *a,b*) | Decrease | Decrease | Decrease |
| Cleworth and Edman (1972)* | — | — | Decrease |
| Kawai and Kuntz (1973) | No change‡ | — | Decrease |
| Fujime (1975)* | Small change | Decrease/increase§ | Decrease |
| Paolini et al. (1976)* | Increase/decrease‖ | — | Decrease |
| Paolini et al. (1977)* | — | — | Decrease |
| Halpern (1977)* | — | — | Decrease |
| Zite-Ferenczy & Rudel (1978)* | — | — | Decrease |

Comparison of previous measurements of intensity changes in the first- and second-order lines.
*Used single fibers.
‡Used variable slit width, fixed slit showed an increase.
§Minimum at 3.0 $\mu$m for single fiber.
‖Peak at 3.0 $\mu$m for single fibers.

and analyses used by each investigator. We attribute our present results to the improvements in our recording and computer analysis systems, particularly our collection of the diffraction line from a much larger portion of the diffraction cone. Another important factor has been our use of single fibers. Diffraction patterns from whole muscle are not as sharp as those observed using single fibers. Fiber misalignment doubtless contributes to this more diffuse pattern. Slight differences in $S$ from fiber to fiber would also contribute to a more diffuse pattern. For these reasons we feel that the single fiber patterns are more easily analyzed. (Our earlier investigations using single fibers had also revealed some variation in the intensity of the first-order line with $S$.

The first-order length-intensity relationship exhibits remarkable consistency and linearity (Table II). There were few experiments that did not demonstrate a good fit to least squares regression analysis. The second order also demonstrates consistent regression data. The absolute magnitude of the second-order diffraction intensity is substantially less than for the first order, but rises more rapidly as the muscle is passively stretched.

Chemically skinned and fully glycerinated fibers were used to investigate the effect of altered or removed membrane systems on the diffraction pattern. The contractile apparatus apparently remains intact and functional. The fact that the first- and second-order length-intensity relationships from all preparations are not significantly different indicates that the membrane components of muscle have little or no effect upon the diffraction phenomenon.

It is also interesting to note that most earlier studies did indicate a decrease in the intensity of the first-order line upon muscle activation. This is such a profound phenomenon that it appears not to matter much what muscle preparation or detector system is used. We also found that chemically skinned fibers demonstrate this significant intensity decrease. The second-order intensity also decreases but its significance is masked by the steep resting intensity curve. Furthermore, past studies have indicated that non-uniformity in $S$ of different fibers as well as lateral misalignment of fibers makes the results of stimulated whole muscle or muscle bundle studies difficult to interpret.

We have examined two model systems in an attempt to find a theoretical basis for our results. The first, involving a one-dimensional diffraction grating model, is found to be inadequate. The second model, one which successfully predicts our experimental results, is discussed in a following section.

*Striated Muscle as a One-Dimensional Diffraction Grating*

In the first model we examine the application of the standard grating equation to a single striated muscle fiber. In this model, $b$ is the width of the $I$-band. The intensity ($I$) for a given order ($n$) is given by the following equation:

$$I = A_0^2 \frac{\sin^2\beta}{\beta^2} \frac{\sin^2 N\gamma}{\sin^2\gamma}, \tag{1}$$

where:

$$\gamma = \pi S \sin\theta/\lambda$$

$$\beta = \pi b \sin\theta/\lambda$$

$$A_0 = ab/x$$

$$n\lambda = S \sin\theta,$$

where $\theta$ is the diffraction angle, and $x$ is the distance from the fiber to the recording device, and $a$ is the wave amplitude.
For $\gamma = 0, \pi, 2\pi$,

$$\frac{\sin^2 N\gamma}{\sin^2 \gamma} \rightarrow N^2 \tag{2}$$

therefore,

$$\frac{I_1}{(a/x)^2} = b^2 N^2 \frac{(\sin \pi b/S)^2}{(\pi b/S)^2}, \tag{3}$$

and

$$\frac{I_2}{(a/x)^2} = b^2 N^2 \frac{(\sin 2\pi b/S)^2}{(2\pi b/S)^2}. \tag{4}$$

A plot of Eqs. 3 and 4 as a function of $S$ is presented in Fig. 5. Both first- and second-order line intensities show a $S$ dependence; however, the order of magnitude of the dependence as well as the direction are quite different. The first-order line intensity increases with increasing $S$ up to a value of 3.3 $\mu$m after which it decreases slightly. The range of the intensity change is less than twofold. It varies from two to six times the intensity of the second-order line.

Second-order line intensity decreases with increasing $S$ to ~3.2 $\mu$m and increases slightly thereafter.

These variations in first- and second-order line intensity predicted from the transmission grating analysis do not agree with our measurements. In particular, the grating analysis predicts a large increase of $I_1$ in the range of 2.2 to 2.6 $\mu$m. Our results (Fig. 2) show a very small increase in this range. The second-order line intensity, which is predicted to fall significantly in this range, in fact shows a rise. Similarly in the range from 3.2 to 3.6 $\mu$m $I_1$ is predicted to fall slightly. The experimental result is the opposite and shows a continuing and substantial increase in $I_1$ with $S$. It must therefore be concluded that the transmission grating, based as it is upon a one-dimensional model, is not adequate to explain the data. (Not excluded, however, is the possibility that a more intricate model, one that allowed for the presence of Z lines, M lines, and H zones, could be devised and would better fit the experimental data. In view of our work and the note of Rudel and Zite-Ferenczy [1978] in which they argue that effects they have observed are difficult to explain on the basis of the fiber behaving as a plane grating, we believe that a three-dimensional approach offers a better basis for a comprehensive theory.)

Another way of looking at a one-dimensional model of a muscle fiber is to use the unit cell approach of Fujime (1975). Expressions for the "molecular" scattering factors of the thin and thick filaments were derived and the scattered amplitude from a fiber containing N + 1 unit cells was determined. The intensity, $I_n$, of the $n$th-order reflection is proportional to the square of the scattered amplitude and was calculated for various $S$.

In the range of $S$ between 2.2 and 3.6 $\mu$m the intensity of the first-order line ($I_1$) was predicted to increase by ~15%. Although this small increase appeared to agree with Fujime's experimental observations, we have found a far greater dependence of $I_1$ on $S$. This model does not agree with our data even if different values are chosen for the density of scatterers $n_A$ ($A$-band) and $n_I$ ($I$-band).

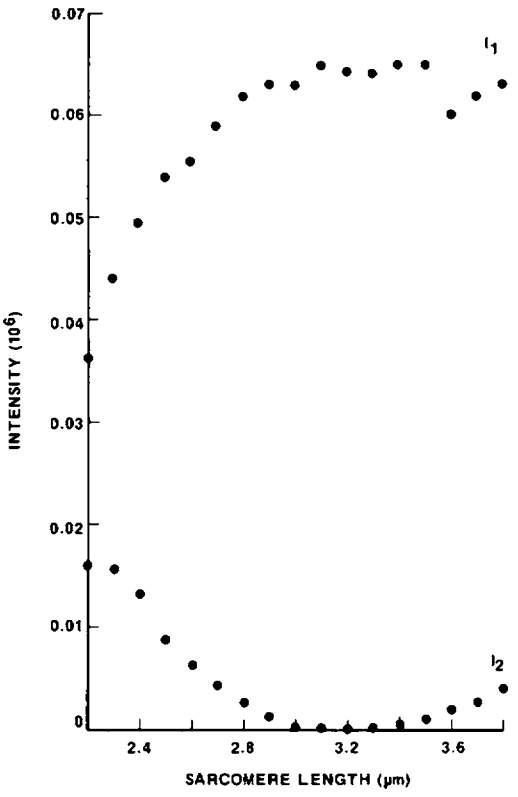


FIGURE 5

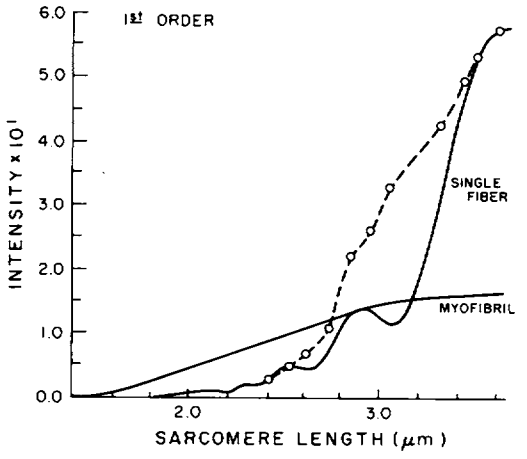


FIGURE 6

FIGURE 5 Dependence of first-order line intensity ($I_1$) and second-order line intensity ($I_2$) upon $S$ as determined using the grating equation:

$$I = A_0^2 \frac{\sin^2\beta}{\beta^2} \frac{\sin^2 N\gamma}{\sin^2\gamma}$$

Intensity units are arbitrary.

FIGURE 6 Intensity of the first-order diffraction peak vs. $S$ for the model where only $A$- and $I$-bands are considered. Experimental data was replotted (---0---). The experimental intensity was normalized at $S$ = 3.5 μm. The single fiber radius was taken as $a$ = 50 μm. The accompanying plot of intensity vs. $S$ for myofibril $a_0 = a/100$ showed much smaller intensity variation over the experimental range of $S$ values.

### *Three-Dimensional Model*

The inability of the simple linear grating to explain our observed results on the intensity variation with $S$ leads us to suggest that the muscle diffraction problem may require a more complete three-dimensional treatment. A thick grating composed of a bundle of myofibrils will provide additional diffraction effects besides those commonly considered. Physically, light that propagates in a particular direction will now experience further optical path differences depending on the region of the sarcomere traversed. These differences in optical path lengths will, upon linear superposition, lead to the compounding of the simple linear grating effect.

A convenient model for such a thick grating is the scaled-up version of the model used by Bear and Bolduan (1950) to explain x-ray diffraction from collagen fibers. The main result is given by:

$$I_\ell = I_0 |\delta E_{0\ell}|^2 [F_\ell(q_\rho a)]^2 \left\{ G_\ell \left[ (q_z - \ell K) \frac{p}{2} \right] \right\}^2, \tag{5}$$

where $I_\ell$ is the intensity of the $\ell$th diffraction order, $I_0$ is the single element scattering intensity, and $|\delta\epsilon_{0\ell}|$ is the magnitude of the dielectric fluctuation of the $\ell$th order. Diffraction effect in the equatorial plane is provided by $F_\ell(q_\rho a)$, where

$$F_\ell (q_\rho a) = 2\pi a^2 \frac{J_1(q_\rho a)}{q_\rho a}. \tag{6}$$

Here $a$ is the radius of the diffracting cylinder, either the myofibril or the single fiber; $q_\rho$ is the equatorial component of the scattering wave vector; $J_1(x)$ is the Bessel function of the first order for the argument $X$.

The factor $G_\ell$ $[(q_z - \ell k)\ p/2]$ is the normally considered meridional or $z$-direction diffraction effect.

$$G_\ell \left[ (q_z - \ell k) \frac{p}{2} \right] = \frac{p \sin \left[ (q_z - \ell K) \frac{p}{2} \right]}{\left[ q_z - \ell K) \frac{p}{2} \right]}, \tag{7}$$

with $p$ being the illumination diameter of the laser beam, $q_z$ the $z$-component of the scattering wave vector, and $K = 2\pi/S$.

Two additional features have been incorporated in our model. First of all, because it has been well established that the $S$ and cross section are related by the constant sarcomere volume $V_0$ (Huxley, 1953), $S$ and $a$ are related by:

$$a = \left[ \frac{V_0}{\pi S} \right]^{1/2}. \tag{8}$$

Second, the wide equatorial collection scheme employed in our experiment is accounted for by an integration over all relevant $q_\rho$ values.

Results of the present analysis are compared with experimental data in Figs. 6 and 7, for the first- and second-order diffraction intensities, respectively. In Fig. 6 the muscle fiber is assumed to have only two distinguishing indices, the $A$ and $I$ bands. It is noted that, far from being a constant, the first-order intensity rises sharply as a function of the $S$. There exists, however, distinctively, a superimposed oscillatory pattern in $I_\ell$ as the $S$ value is changed. This behavior is characteristic of a three-dimensional grating where interference can take place not only by traversing through the medium at different angles, but also by beams of light being subjected to different velocities of propagation even when traversing along the same direction.

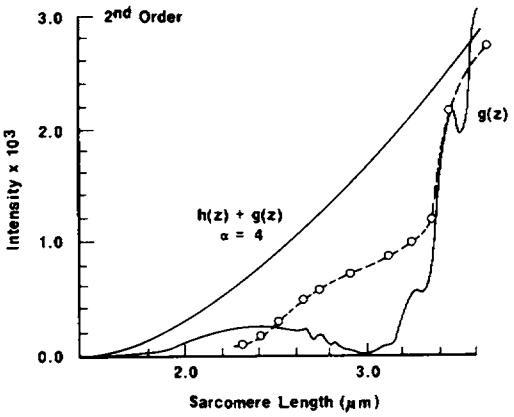


FIGURE 7 Intensity of second-order diffraction peak vs. $S$ for two models. $g(z)$: Only $A$- and $I$-bands contributed to the diffraction grating. $h(z) + g(z)$: Z membrane and the H zone have been incorporated in an idealization of more complex grating. $\alpha = 4$ implies that the dielectric fluctuation from Z membrane is assumed to be 4 times that of the H zone.

The comparison with experimental data of the first-order line is shown in Fig. 6. In particular, we notice the trend of increasing intensity of the first order upon increasing $S$ in both the theory and the experiment.

It is further shown here that should the basic scattering element of the muscle fiber be of the (myofibril) dimension ($a_0 \simeq 0.5$ μm), then the observed intensity dependence on sarcomere length obtained does not occur theoretically. A comparison of the intensity dependence on $S$ for these two cases is also provided in Fig. 6. Our data thus suggests convincingly that the basic scattering unit in the resting single fiber is of cross sectional dimension of the fiber, not the myofibril. Our results in the case of the active fiber (Fig. 4), however, show a reduced length dependency of $I_1$. This data fits, rather closely, the myofibril model in Fig. 6. Thus we argue that the basic scattering element in the active muscle is on the order of the myofibril. This is in agreement with the results of Bonner and Carlson (1975), wherein they concluded that (for active muscle) the "dominant light-scattering elements have the dimensions of the myofibrillar sarcomeres or their $A$ and $I$ band subunits."

The comparison between theory and experiment for the second-order line (Fig. 7) shows that the general trend of increasing $I_2$ as $S$ is lengthened still persists. There is, however, a disquieting effect predicted by the theory for $I_2$ at $S = 3.0$ μm when only $A$ and $I$ bands are considered (trace with $g[z]$). This theoretical result has also been obtained by Fujime (1975) using the linear grating model. The large discrepancy between theory and experiment has led us to suggest that second-order pattern may be more sensitive to other structures of the sarcomere. Indeed, even extremely crude representations of the Z membrane and the H zone alter the theoretical results greatly. Shown also in Fig. 7 is the situation where the Z membrane is represented by a sharp spike of refractive index change, and the H zone is represented by a sharp decrease of index of refraction. Together they represent the added factor of $h(z)$. The inclusion of these elementary model additions to the sarcomere structure removes the zero intensity point at $S = 3.0$ μm.

*X-Ray Diffraction Studies*

A number of investigators have shown that the ratio of the intensities of the 1,0 and 1,1 equatorial reflections of a live, resting muscle depend upon its $S$ (Elliott et al., 1963; Huxley, 1968; Rome, 1972; Haselgrove and Huxley, 1973). As $S$ increases, the ratio of the intensities I(1,0):I(1,1) increases. These and other studies have also shown that the lattice spacing $d(1,0)$ is a function of $S$, decreasing with increasing $S$.

The decrease in lattice spacing $d(1,0)$ is a direct result of the isovolumic behavior of a muscle fiber. Since the thick filaments are closer together at longer $S$, the density of scattering in the $A$-band is increased, resulting in an increase in the scattering power of the $A$-band. (This behavior has been incorporated into our theoretical development.) It would clearly be one factor causing the increase in intensity of the first-order diffraction line with increase in $S$ which we report in this paper.

The dependence of the ratio of the intensities of the (1,0) and (1,1) equatorial reflections upon $S$ (resting muscle) has been interpreted as resulting from a decrease in the mass of actin at the trigonal positions of the myosin lattice (Haselgrove, 1975). This decrease in mass would also result in a decrease in scatterers in the $A$-band and would tend to decrease the diffracting power of the $A$-band. This must, however, be more than offset by the increase in diffracting power resulting from the decrease in the (1,0) spacing.

The situation is different in a stimulated muscle fiber. In this case I(1,0):I(1,1) decreases relative to its value at rest. This has been interpreted as indicating radial cross-bridge movement toward the actin filaments in the trigonal position. Could such movement affect the diffracting power of the $A$-band and provide an explanation for the increase in intensity of the first-order line which is observed upon stimulation? Any change in diffracting power of the $A$-band resulting from such movement would have to result either from the alteration in position of scatterers (because their total number does not change) or from a change in form birefringence (because our incident light is polarized).

The decrease in first-order line intensity upon stimulation could also result from lateral misalignment of myofibrils. Indeed, our model (Fig. 6) predicts an intensity decrease in $I_1$ for a shift in basic scattering element from a single fiber to the order of a myofibril. The predicted intensity change is observed (Fig. 4). Skewing of the fiber striations ($A$- and $I$-bands) could be caused by misalignment of myofibrils during muscle activation. Myofibrillar misalignment has been observed by Hill (1977) in the course of her studies on active muscle fibers using an interference microscope. It may form the basis of the observed changes in line intensity during activation.

## CONCLUSION

This study has revealed the following: (*a*) The intensity of the first-order diffraction line from a single muscle fiber shows a strong dependence on $S$. (*b*) Increasing the $S$ in a resting fiber results in an increase in the intensity of the first-order line. (*c*) Stimulation results in a decrease in intensity of the first-order line. This decrease is greater at longer $S$. (*d*) Neither an analysis based on a diffraction grating with variable spacing nor the unit cell model of Fujime provide an explanation for the observed dependency of first-order line intensity upon $S$. (*e*) Due to the isovolumic nature of a muscle fiber, the volume density of scatterers (thick

filaments) increases with increasing $S$. This has the effect of increasing the scattering power of each $A$-band. ($f$) The origin of the intensity decrease upon stimulation is now known. We have suggested that it could result from lateral misalignment of myofibrils, which often occurs upon activation.

We are indebted to Professor Sir A. F. Huxley for his suggestions on the importance of collecting as large a portion of the diffraction cone as possible. The optical system as discussed in the Appendix was designed by Mr. Paul A. Roos.

The authors would like to express their appreciation to the National Science Foundation (PCM-7903256 to Dr. Baskin) and the National Science Foundation (PCM 77-08371 to Dr. Yeh) for their financial support.

*Received for publication 30 November 1978 and in revised form 29 May 1979.*

## APPENDIX

### *Optical system*

The optical system is a second generation design based on experience with another diffractometer optical system that collected and transmitted diffracted light to a maximum half-angle of 25° and scattered light to 10° (Paolini et al., 1976).

To increase the acceptance angle to 30° for diffracted light and to at least 60° for scattered light, a radically different approach was necessary.

Microscope optical systems of the immersion type satisfy the angular requirements since a 1.40 numerical aperture system operates at a 67.3° half angle in a medium having an index of refraction of ~1.52. Most immersion objectives of 1.40 na have a working distance of ~0.25 mm, which precludes convenient use in this application.

The corresponding 1.40-na condenser systems, however, operate at the same aperture and provide a working distance of 1.65 mm in glass and oil, and in this case can be used in the reverse direction as a collector.

A preliminary study of a 1.40 na achromatic condenser was made to check the effects of the use of water or saline as an immersant instead of immersion oil and glass. This showed that a working distance of slightly less than half the design distance for oil/glass was optimum for saline immersion.

A fan of rays was traced from a point 0.72 mm in saline from the entrance surface of the achromatic condenser through its various elements with the results shown in Fig. 8. Here we see that at a distance of 80 mm from the last surface of the collector/condenser, a 30-mm free aperture will transmit all the light

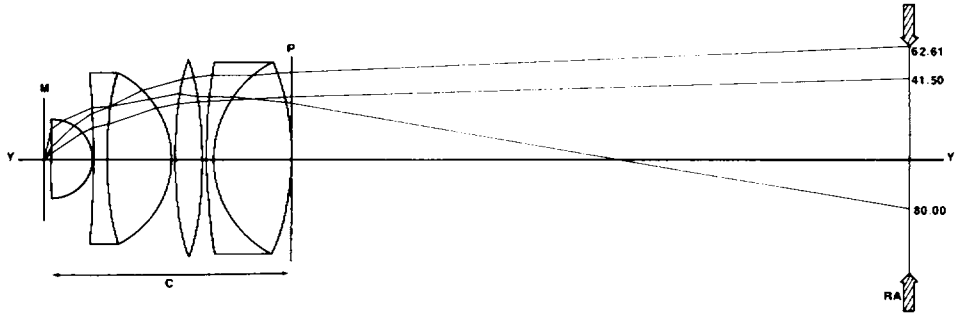


FIGURE 8 Condenser/collector raytrace diagram (submitted twice actual size): The collector, C, lies on the optical axis, Y. 3 rays (41.5°, 62.61°, and 80.0°) from the muscle preparation M are traced through each of the 10 surfaces of the 4-element collector and out 80 mm to the relay aperture, RA, of 30 mm. The relay optics focus upon the plane, P.

collected out to the maximum half angle of 80.0°. Note that the light collected beyond 62.6° is refracted to such an extent that its slope becomes negative. This is the result of spherical aberration caused by working in a different immersion medium (Ringer's solution) and at a different working distance than that for which the system was designed.

From the same raytrace data, the relationship of input angle (either diffraction or scattering) to the height above the axis in a plane tangent to the vertex of the last surface of the collector can be calculated. Fig. 9 shows this to be linear ($h' = 0.2042\ \alpha + 0.0715$; $r^2 = 0.9996$) out to ~36°, which is far greater than what is required for measurement of the first and second-order diffraction angles of muscle preparations. Therefore, by focusing on this plane with an appropriate relay system, we can image the position of the exit beams upon the sensor for display and recording of diffraction angle data.

Scattered light emerges from the preparation as cones of light with the cone axis perpendicular to the optical axis and parallel to the plane entrance surface of the collector. Therefore, the trace of the intersection of the cone on the entrance surface is an hyperbola. This fact was used for calculating the position of the entrance rays in the following analysis. A cone of rays was traced through the collector with the results shown in Fig. 10. Note that the plot of output height due to scattering is almost a straight line instead of an hyperbola and is perpendicular to the displacement due to diffraction. This most beneficial distortion is caused by the same spherical aberration previously mentioned. The collector accepts up to a 78.8° half angle of the scattering cone at the illustrated 26.56° diffraction angle. This angle is measured from the optical axis to the ray in question in the $X=Y$ plane with the cone axis at the center. This corresponds to the 80.0° collection half angle maximum in the plane of the raytrace.

Further studies were made to determine the effects of a change in working distance and decentering of the collector upon output linearity. It was found that the normalized height at the output of the collector

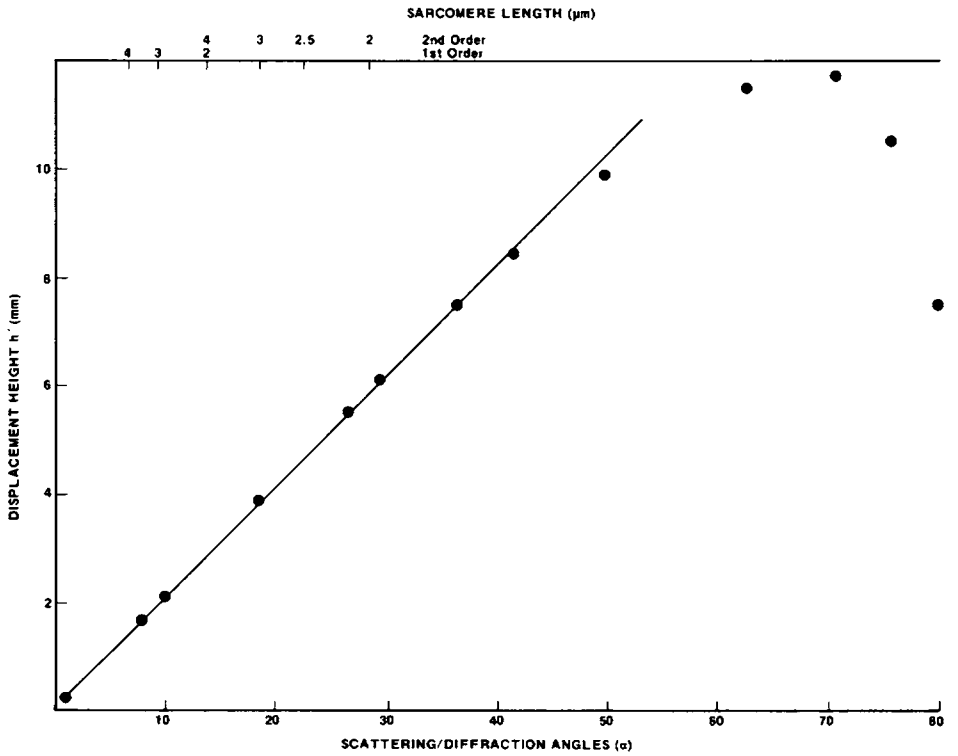


FIGURE 9 Input angle/output height diagram: The input angle $\alpha$ and its corresponding $S$ is plotted vs. output displacement height $h'$ at the back of the collector.

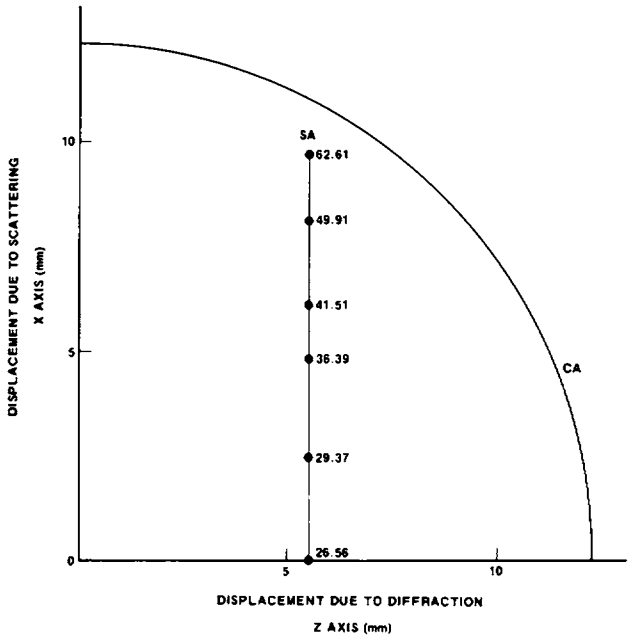


FIGURE 10 Diffraction line output: A calculated diffraction line representation for one quadrant of the exit plane of the collector aperture CA is illustrated. The 26.56° diffraction angle shown is equivalent to a second-order $S$ of 2.12 $\mu$m. Five scattering angle, SA, values demonstrate the straight line shape of the output.

was linear for working distances between 0.7 and 1.3 mm. Thus, limited vertical movement of the muscle fiber will not affect the diffraction data during an experiment. However, lateral decentering of the collector by as little as 0.0732 mm from the $\phi$ order optical axis will shift the output axis by 0.08316 mm. To eliminate this potential problem, the collector is precisely mounted on the chamber top with locating pins.

To use the output of this collection system, a relay system is required that provides approximately unit magnification in the direction of displacement due to diffraction. At 90° to this direction, a very short focal length stigmatizer system is needed to concentrate the line images of scattered light into points. The resultant series of points (one for each diffracted order) contain essentially all the transmitted diffraction light. Such an optical system (anamorphic) is comprised of cylindrical lenses of appropriate focal length and spacing with axes 90° apart.

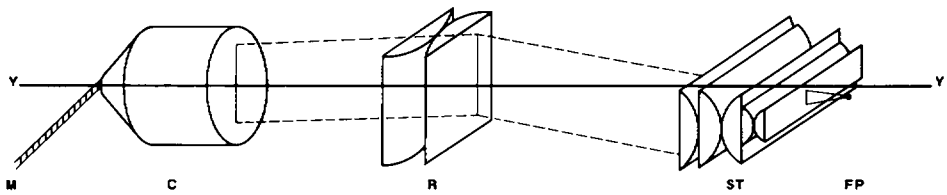


FIGURE 11 Optical system-isometric view: The laser irradiates the muscle preparation, M, along the optical axis, Y. A diffracted order emerging from the collector, C, is focused upon the relay cylinders, R, which magnify or diminish the diffraction angle displacement along the Z axis. The stigmatizing cylinders, ST, image the scattered light along the X axis into a point at the focal plane FP where the CCD sensor is placed.

Fig. 11 shows an isometric view of the complete optical system showing a path of diffracted and scattered light through each element. Note that both the relay and stigmatizer optics act as plane parallel plates of glass having no power in one direction. For experiments described in this manuscript, the system used an 8.9-mm focal length Bausch and Lomb achromatic condenser (1.40 na). The relay system, comprised of two cylindrical lenses with an effective 22-mm f.l., is located 30–60 mm above the collector. Five cylindrical lenses with a combined thick lens 11.8 mm focal length make up the stigmatizer system located another 20–50 mm along the optical axis. The CCD sensor is placed at the focal point above the stigmatizer system (≃ 5–10 mm) to collect the imaged diffraction data.

## REFERENCES


BEAR, R. S., and O. E. A. BOLDUAN. 1950. Diffraction by cylindrical bodies with periodic axial structure. *Acta Cryst.* **3**:236–241.

BONNER, R. F., and F. D. CARLSON. 1975. Structural dynamics of frog muscle during isometric contraction. *J. Gen. Physiol.* **65**:555–581.

BUCHTHAL, F., and G. G. KNAPPEIS. 1940. Diffraction spectra and minute structure of the cross-striated muscle fiber. *Skand. Arch. Physiol.* **83**:281–307.

CLEWORTH, D. R., and K. A. P. EDMAN. 1972. Changes in sarcomere length during isometric tension development in frog skeletal muscle. *J. Physiol. (Lond.)* **227**:1–17.

ELLIOTT, G. F., J. LOWRY, and C. R. WORTHINGTON. 1963. An x-ray and light-diffraction study of the filament lattice of striated muscle in the living state and in rigor. *J. Mol. Biol.* **6**:295–305.

FORD, L. E., A. F. HUXLEY, and R. M. SIMMONS. 1977. Tension responses to sudden length change in stimulated frog muscle fibers near slack length. *J. Physiol. (Lond.)* **269**:441–515.

FUJIME, S. 1975. Optical diffraction study of muscle fibers. *Biochim. Biophys. Acta.* **379**:227–238.

HALPERN, W. 1977. A rapid, on-line, high resolution analyzer of striated muscle diffraction patterns. *Proc. S. D. Biomed. Symp.* **16**:429–439.

HASELGROVE, J. C. 1975. X-ray evidence for conformational changes in the myosin filaments of vertebrate striated muscle. *J. Mol. Biol.* **92**:113–143.

HASELGROVE, J. C., and H. E. HUXLEY. 1973. X-ray evidence for radial cross-bridge movement and for the sliding filament model in actively contracting skeletal muscle. *J. Mol. Biol.* **77**:549–568.

HILL, D. K. 1953*a*. The optical properties of resting striated muscle. The effect of rapid stretch on the scattering and diffraction of light. *J. Physiol. (Lond.)* **119**:489–500.

HILL, D. K. 1953*b*. The effect of stimulation on the diffraction of light by striated muscle. *J. Physiol. (Lond.)* **119**:501–512.

HILL, L. 1977. A-band length, striation spacing and tension change on stretch of active muscle. *J. Physiol. (Lond.).* **266**:677–685.

HUXLEY, H. E. 1953. X-ray analysis and the problem of muscle. *Proc. R. Soc. Lond. B. Biol.* **141**:59–62.

HUXLEY, H. E. 1968. Structural difference between resting and rigor muscle; evidence from intensity changes in the low-angle equatorial x-ray diagram. *J. Mol. Biol.* **37**:507–520.

JULIAN, F. J. 1971. The effect of calcium on the force-velocity relation of briefly glycerinated frog muscle fibers. *J. Physiol. (Lond.).* **218**:117–145.

KAWAI, M., and J. D. KUNTZ. 1973. Optical diffraction studies of muscle fibers. *Biophys. J.* **13**:857–876.

PAOLINI, P. J., R. J. BASKIN, K. P. ROOS, and J. W. CLINE. 1976. Dual-channel diffractometer utilizing linear image sensor charge-coupled devices. *Rev. Sci. Instrum.* **47**:698–702.

PAOLINI, P. J., K. P. ROOS, and R. J. BASKIN. 1977. Light diffraction studies of sarcomere dynamics in single skeletal muscle fibers. *Biophys. J.* **20**:221–232.

PAOLINI, P. J., R. SABBADINI, K. P. ROOS, and R. J. BASKIN. 1976. Sarcomere length dispersion in single skeletal muscle fibers and fiber bundles. *Biophys. J.* **16**:919–930.

RANVIER, J. 1874. Du spectre produit par les muscles stries. *Arch. de Physiol.* **T6**:774–775.

ROME, E. 1972. Relaxation of glycerinated muscle: low-angle x-ray diffraction studies. *J. Mol. Biol.* **65**:331–345.

RÜDEL, R., and F. ZITE-FERENCZY. 1978. Bragg-reflexion of light by cross-striated frog muscle. *J. Physiol.* **284**:99-100P.

SANDOW, A. 1963*a*. Diffraction patterns of the frog sartorius and sarcomere behavior under stretch. *J. Cell. Comp. Physiol.* **9**:37–54.

SANDOW, A. 1936*b*. Diffraction patterns of the frog sartorius and sarcomere behavior under contraction. *J. Cell. Comp. Physiol.* **9**:55–75.

TAYLOR, D. L. 1976. Quantitative studies on the polarization optical properties of striated muscle. *J. Cell. Biol.* **68**:497–511.

ZITE-FERENCZY, F., and R. RUDEL. 1978. A diffractometer using a lateral effect photodiode for the rapid determination of sarcomere length changes in cross-striated muscle. *Pfluegers Archiv. Gesamte Physiol. Menschen Trere.* **374**:97–100.